ARTICLE

BIOTECHNOLOGY and BIOENGINEERING

A Systems Biology Approach to Study Glucose Repression in the Yeast *Saccharomyces cerevisiae*

Steen Lund Westergaard, Ana Paula Oliveira, Christoffer Bro, Lisbeth Olsson, Jens Nielsen

Center for Microbial Biotechnology, BioCentrum, Technical University of Denmark, Building 223, DK-2800 Kgs. Lyngby, Denmark; telephone: +45 4525 2696; fax: +45 4588 4148; e-mail: jn@biocentrum.dtu.dk

Received 6 February 2006; accepted 13 July 2006

Published online 28 July 2006 in Wiley InterScience (www.interscience.wiley.com). DOI 10.1002/bit.21135

ABSTRACT: Glucose repression in the yeast *Saccharomyces cerevisiae* has evolved as a complex regulatory system involving several different pathways. There are two main pathways involved in signal transduction. One has a role in glucose sensing and regulation of glucose transport, while another takes part in repression of a wide range of genes involved in utilization of alternative carbon sources. In this work, we applied a systems biology approach to study the interaction between these two pathways. Through genome-wide transcription analysis of strains with disruption of *HXK2*, *GRR1*, *MIG1*, the combination of *MIG1* and *MIG2*, and the parental strain, we identified 393 genes to have significantly changed expression levels. To identify co-regulation patterns in the different strains we applied principal component analysis. Disruption of either *GRR1* or *HXK2* were both found to have profound effects on transcription of genes related to TCA cycle and respiration, as well as ATP synthesis coupled proton transport, all displaying an increased expression. The *hxk2Δ* strain showed reduced overflow metabolism towards ethanol relative to the parental strain. We also used a genome-scale metabolic model to identify reporter metabolites, and found that there is a high degree of consistency between the identified reporter metabolites and the physiological effects observed in the different mutants. Our systems biology approach points to close interaction between the two pathways, and our metabolism driven analysis of transcription data may find a wider application for analysis of cross-talk between different pathways involved in regulation of metabolism.

Biotechnol. Bioeng. 2007;96: 134–145.

KEYWORDS: carbon catabolite repression; transcription analysis; integrative analysis; PCA; reporter metabolites; signal transduction

Introduction

Glucose repression in the yeast *Saccharomyces cerevisiae* involves several different signal transduction pathways activated both by extracellular glucose levels and by intracellular levels of yet un-identified metabolites and/or fluxes through key enzymes. Due to the complex regulatory structure, the mechanisms of glucose repression has served as a paradigm for studying nutrient sensing and regulation, and there are many studies focusing on the role of the individual components in the various pathways (Ahuatzi et al., 2004; Dombek et al., 2004; Flick and Johnston, 1991; Lascaris et al., 2004; Moreno et al., 2005; Newcomb et al., 2003; Nigavekar et al., 2002; Özcan, 2002; Palomino et al., 2005; Polish et al., 2005; Rolland et al., 2002; Sanz et al., 2000) (for an extensive review see Gancedo, 1998). In recent years, a small number of genome-wide transcription studies have been performed to analyze the effects of disrupting or over-expressing individual components involved in glucose repression (Lascaris et al., 2002; Westergaard et al., 2004).

Figure 1 gives a simplified overview of two of the main pathways involved in glucose repression, with indication of a few key proteins taking part in these pathways. In one pathway, the extracellular glucose concentration is sensed by two proteins, Snf3p and Rgt2p. Snf3p has a high affinity for glucose and acts as a sensor at low glucose concentrations, whilst Rgt2p has low affinity for glucose and functions primarily as sensor at high glucose concentrations (Özcan and Johnston, 1999; Schmidt et al., 1999). The signal triggered by these sensors results in expression of different hexose transporters (encoded by *HXT* genes). The details of this pathway have been almost completely elucidated (Flick et al., 2003; Kaniak et al., 2004; Kim et al., 2003; Lakshmanan et al., 2003; Li and Johnston, 1997; Moriya and Johnston, 2003; Mosley et al., 2003; Özcan et al., 1996; Polish et al.,

This article contains Supplementary Material available via the Internet at http://www.interscience.wiley.com/jpages/0006-3592/suppmat

Christoffer Bro's present address is NatImmune A/S, Fruebjerg 3 Box 3, DK-2100 Copenhagen, Denmark.

Correspondence to: J. Nielsen

Contract grant sponsor: Danish Biotechnology Instrument Center (DABIC)

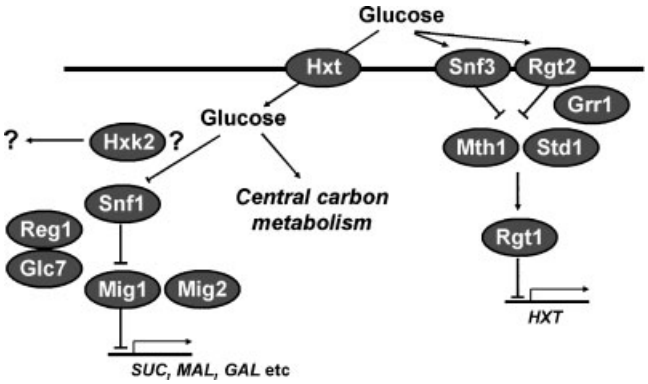

Figure 1. Key components of the two most important pathways involved in glucose repression. The glucose signal is mediated across the cell membrane via the receptors Rgt2 and Snf3. Transport of glucose is carried out by hexose transporters encoded by *HXT* genes. At high glucose concentration, Grr1 deactivates Rgt1-repression of *HXT*-genes. Additionally, Grr1 plays a role in sensing of other nutrients, such as amino acids and regulation of uptake thereof. Inside the cell, Hxk2 catalyses phosphorylation of glucose to glucose-6-phosphate (Glucose-6-P), and may be involved in inactivation of the Snf1 complex. This inactivation is catalyzed by the protein phosphatase Glc7-Reg1. When dephosphorylated, Mig1 enters the nucleus and here it takes part in promoter binding resulting in repression of several genes. Derepression occurs when Mig1 is phosphorylated by Snf1.

2005; Westergaard et al., 2004), and it has been shown that the ubiquitin-protein ligase Grr1 plays a role in inactivation of key proteins of this pathway (Flick et al., 2003), probably through ubiquitination (and, consequently, targeting them to proteolysis) (Moriya and Johnston, 2003; Oesterhelt et al., 2003).

In the other pathway, often referred to as the main glucose repression pathway, the DNA-binding protein Mig1 plays a key role. The sensor of this pathway is not yet known, but it is believed to involve hexokinase 2 (Hxk2, a glycolytic enzyme), which may communicate the presence of intracellular glucose further down in the pathway. The protein kinase Snf1 and the protein phosphatase Glc7 are likely to be recipients of this signal (Mayordomo and Sanz, 2001; Randez-Gil et al., 1998), probably through three kinases upstream of Snf1 (Kuchin et al., 2003; Nath et al., 2003; Sutherland et al., 2003). When the cell senses low levels of glucose, Snf1 is activated through a phosphorylation, and the active Snf1p then catalyzes the phosphorylation of Mig1, causing Mig1p to translocate from the nucleus to the cytosol. Hereby, Mig1-associated repression of several different genes is released. On the other hand, at high levels of glucose, when Snf1 is not phosphorylated, Mig1 remains in the nucleus and here it represses the transcription of genes involved in the metabolism of carbon sources other than glucose and fructose. Additionally to Mig1, Mig2 can also repress transcription of some genes that are Mig1 repressible (e.g., *MAL, GAL*, and *SUC2)*. However, in contrast to Mig1, Mig2 localization does not depend on phosphorylation.

Recently, Kaniak et al. (2004) showed that there is substantial cross-talk between these two pathways. In their study, they combined transcription profiling with chromatic immunoprecipitation and β-galactosidase assays to evaluate which candidate targets are regulated by Rgt1. They also carried out Western analysis to assess abundance of the transcriptional regulators Mig1, Mig2, and Mig3 under different carbon source conditions. Their analyses suggested that a relatively small number of genes are targets of the signaling pathway that functions through Snf3/Rgt2-Rgt1. However, they discovered an elaborate degree of cross-communication between the two major pathways of glucose repression. This is manifested by Mig1 and Mig2 playing a role both in regulation of expression of metabolic genes like *HXT2, HXT4*, and *SUC2*, as well as in regulation of regulatory components like *MIG1*, *SNF3*, and *MTH1*. To date, however, no studies investigating the metabolic effects of deleting several components of the glucose repression pathways in yeast have been reported.

In this work we undertook a systems biology approach to study the role of specific components of the glucose repression pathways. Particularly, we were interested in understanding the effects on metabolism, at physiological and transcriptional levels, of deleting key components of glucose repression. We followed a model guided approach to map those effects onto the metabolic network operating in yeast, namely by using a recently reported method to identify metabolic hot-spots around which most transcriptional changes occur. In our study, we analyzed genome-wide transcription data of four recombinant strains— three single disruptants (*grr1Δ*, *hxk2Δ*, and *mig1Δ*) and one double disruptant (*mig1Δmig2Δ*)—, and their congenic reference strain, under aerobic and glucose repressing conditions. The strains *hxk2Δ*, *mig1Δ*, and *mig1Δmig2Δ* were investigated experimentally here, while *grr1Δ* and the reference strain were previously characterized by us in Westergaard et al. (2004). Since we also aimed at performing a comparative transcriptional profiling of the various mutants, we included the reference strain and *grr1Δ* data in the present analysis.

Materials and Methods

Strains and Preculture

Three strains from CEN.PK background were used in this study, derived from the reference strain CEN.PK-113-7D. The reference strain and one additional mutant also analyzed in this study were previously characterized in Westergaard et al. (2004). The genotypes of the reference strain and all the mutants are listed in Table I. The CEN.PK513-3A and the CEN.PK520-6B strains are courtesy of Dr. P. Kötter, J. W. Goethe-University, Frankfurt, Germany.

The strains were stored at −80°C suspended in yeast extract peptone dextrose (YPD)-medium containing a volumetric fraction of 15% glycerol. Before each experiment, cells from the stock were transferred to YPD plates.

Table I. Strains employed in the study.

Strain	Genotype	Strain origin	Experimental data
CEN.PK113-7D Reference strain (IBT 100.014)	*MATa URA3 HIS3 TRP1 LEU2 MAL2-8^c SUC2*	Dr. P. Kötter, J. W. Goethe-University, Frankfurt, Germany	Westergaard et al. (2004)
CEN.PK513-3A *grr1Δ* (IBT 100.012)	*MATa grr1::loxP-KanMX-loxP MAL2-8^c SUC2*	Dr. P. Kötter, J. W. Goethe-University, Frankfurt, Germany	Westergaard et al. (2004)
CEN.PK520-6B *hxk2Δ* (IBT 100.008)	*MATa hxk2::loxP-Kan-loxP MAL2-8^c SUC2*	Dr. P. Kötter, J. W. Goethe-University, Frankfurt, Germany	This study
T468 *mig1Δ* (IBT 100.004)	*MATa mig1::MEL1 MAL2-8^c SUC2*	Klein et al. (1999)	This study
T475 *mig1Δmig2Δ* (IBT 100.000)	*MATa ura3 mig1::MEL1 mig2::URA3 MAL2-8^c SUC2*	Klein et al. (1999)	This study

The plates were incubated for 2 days at 30°C, after which they were stored at 4°C. For inoculation of the preculture, a single colony from the YPD-plates was used. A minimal medium with glucose as the sole carbon source, was used for the precultures (Verduyn et al., 1992). The exact amounts per liter of the compounds were $(NH_4)_2SO_4$, 7.50 g; KH_2PO_4, 14.40 g; $MgSO_4 \cdot 7H_2O$; 0.50 g; D-glucose, 10.0 g; Antifoam 289 (A-5551, Sigma-Aldrich, St. Louis, MO), 0.050 mL; trace metals, 2.0 mL (composition given below); vitamins, 0.1 mL (composition given below). The trace metal solution contained per liter: EDTA (Titriplex III®, Fluka, Buchs, Switzerland), 15.0 g; $ZnSO_4 \cdot 7H_2O$, 4.5 g; $MnCl_2 \cdot 2H_2O$, 0.82 g; $CoCl_2 \cdot 6H_2O$, 0.3 g; $CuSO_4 \cdot 5H_2O$, 0.3 g; $Na_2MoO_4 \cdot 2H_2O$, 0.4 g; $CaCl_2 \cdot 2H_2O$, 4.5 g; $FeSO_4 \cdot 7H_2O$, 3.0 g; H_3BO_3, 1.0 g; KI, 0.10 g. The vitamin solution contained per liter: Biotin, 0.05 g; *p*-benzoic acid, 0.20 g; nicotinic acid, 1.00 g; Ca-pantothenate, 1.00 g; pyridoxine HCl, 1.00 g; thiamine HCl, 1.00 g; myo-inositol, 25.00 g.

Glucose was autoclaved separately from the salts and thereafter the glucose and vitamins (sterile filtered) were added aseptically. Two-baffled shake flasks (500 mL) with 100 mL medium were inoculated and incubated for 24 h at 30°C in an orbital shaker at 150 rpm.

Batch Cultivations

The aerobic batch cultivations were carried out in well-controlled 5-L in-house manufactured bioreactors mounted with four metal baffles and with a working volume of 4 L. The growth medium employed in the cultivations was modified from Verduyn et al. (1992). The initial glucose concentration was increased to 40 $g \cdot L^{-1}$ and therefore the concentration of all components, except KH_2PO_4 and antifoam, were three times higher compared to Verduyn et al. (1992). The increase in concentrations of the medium components was made to ensure that the carbon source was the limiting compound (the first medium compound to be exhausted). The medium, therefore, contained per liter: $(NH_4)_2SO_4$, 15.0 g; KH_2PO_4, 3.0 g; $MgSO_4 \cdot 7H_2O$, 1.50 g; D-glucose, 40.0 g; Antifoam 289 (A-5551, Sigma-Aldrich), 0.050 mL; trace metals, 3 mL (composition given above); vitamins, 3 mL (composition given above). From the preculture cells were transferred to obtain an initial OD_{600} between 0.001 and 0.002. Aeration was set to 4 $l \cdot min^{-1}$ (1 atm, 30°C) of atmospheric air and agitation to 750 rpm. The temperature was kept constant at 30°C and pH was maintained at 5.00 ± 0.05 by addition of KOH. The concentration of carbon dioxide and oxygen in the exhaust gas was determined by use of a Brüel and Kjær acoustic gas analyzer (Brüel & Kjær, Nærum, Denmark) (Christensen et al., 1995). We carried out biological independent triplicate cultures for each mutant.

Sampling

For determination of dry weight, substrate and extracellular metabolites, samples were taken at regular time intervals during the cultivations. Samples for determination of substrate and extracellular metabolites were immediately filtered through a 0.45 μm-pore-size acetate filter (CAMEO 25GAS 0.45, Osmonics, Minnetonka, MN) and stored at −20°C, whereas samples for dry weight determination were stored on ice and processed within half an hour.

Samples for whole-genome analysis were taken during the batch experiments when the glucose concentration reached 20 ± 2 $g \cdot L^{-1}$. 20 mL of samples were transferred to 50-mL tubes containing 25 mL crushed ice, so the sample temperature fell below 2°C within 15 s. The cells were pelleted by centrifugation, frozen immediately in liquid nitrogen, and stored at −80°C.

Samples for invertase activity determination were withdrawn at a residual glucose concentration of 20 ± 2 $g \cdot L^{-1}$ during batch cultivations at the same time as the samples for whole-genome expression analysis. A volume corresponding to 40 mg dry weight was sampled from each of the cultivations and centrifuged at 5,000 rpm, 0°C for 5 min. The cells were washed in 10 mM potassium phosphate buffer, 2 mM EDTA, pH 7.5 using the same volume as the sampling volume. The samples were thereafter stored at −20°C in 4 mL of the same buffer.

Biomass Determination

The dry weight formation was determined according to Dynesen et al. (1998) by using 0.45 μm-pore-size nitrocellulose filters (Supor®-450 Membrane Filters, PALL

DOI 10.1002/bit

Life Sciences, Ann Arbor, MI). The OD was determined at 600 nm by using a Hitachi model U-1100 spectrophotometer. The samples were diluted ten times if the absorbance exceeded 0.3. Both in determination of dry weight and OD_{600}, double determinations were made and with very few exceptions, the difference between a set of double determinations was less than 5%. The dry weight measurements form the basis for determination of maximum specific growth rate.

Quantification of Glucose and Extracellular Metabolites

Glucose, ethanol, acetate, glycerol, pyruvate, and succinate were separated and quantified on HPLC using an Aminex HPX-87H column (Biorad, Hercules, CA) (Zaldivar et al., 2002). Subsequent determinations of yield coefficients for extracellular metabolites as well as biomass were based on linear regressions of their concentration as a function of the residual glucose concentration in the exponential growth phase.

Determination of Invertase Activity

The activity of the *SUC2*-encoded invertase was determined in vitro according to Dynesen et al. (1998) with modification as described below. The samples were thawed on ice; cells washed in 4 mL 0.1 M sodium citrate buffer, pH 5.0, and resuspended in 4 mL of the same buffer supplemented with 0.040 mL 0.10 M 1,4-dithiothreitol (DTT). For cell disruption, 0.75 mL glass beads (0.25–0.50 mm in diameter, Jawo Handling, Valby, Denmark) were added to 0.750-mL fractions of cell suspension. The cells were disrupted in a FastPrep bead mill model FP120 Cell Disruptor (Savant Instruments, Holbrook, NY) over 15 intervals of 20 s at speed 5. Between each interval, the cells were cooled on ice. Centrifugation was carried out at 20,000*g*, 0°C for 20 min.

Whole-Genome Transcription Analysis

Total RNA extraction was performed with a FastRNA®, Red Kit (Qbiogene, Illkirch Cedex, France) following manufacturer's instructions, with the exception that the Phenol Acid Reagent solution was replaced by phenol (P-4682, Sigma-Aldrich). cRNA was synthesized as described in the Affymetrix GeneChip® Expression Analysis Manual, after which 15–20 μg were hybridized to Yeast Genome S98 oligonucleotide arrays (Affymetrix, Santa Clara, CA), as described previously (Wodicka et al., 1997). Microarrays were scanned in an Agilent Gene Array Scanner (Affymetrix). Raw-data from GeneChip® Operation Software (Affymetrix) was scaled to the global level of hybridization and normalized (Li and Wong, 2001) to the same level using DNA-Chip Analyzer (dChip, version 1.3, Wong Lab, Harvard School of Public Health and Dana-Farber Cancer Institute, Boston, MA). Expression levels of all 9335 probe sets were calculated with the Perfect Match (PM) model using dChip v1.3 (Li and Wong, 2001). From the 9335 probe sets in the array, the expression level of 6079 annotated unique Open Reading Frames (ORFs) from the *Saccharomyces* Genome Database were extracted. Using the Absent/Present call as calculated by GeneChip® Operation Software, transcripts found to be absent in all arrays were excluded. Hence, the forthcoming analyses were performed on the remaining 5814 transcripts.

Analysis of Variance (ANOVA)

Based on the triplicate transcription data for all the strains tested in this study, we performed a statistical ANOVA test to assess significance of change in expression across all mutants and reference strain. A Bonferroni correction with a global false positive rate of 25% was applied to correct for multiple testing, resulting in a p-value cut-off for significant expression of 4.30×10^{-5}, when investigating the 5814 ORFs that were deemed present on one or more of the arrays in the study on the Yeast Genome S98 oligonucleotide array.

Student's t-test

Additionally, a pair-wise comparison between each mutant and the reference strain was performed using a statistical Student's t-test, to assess the significance of change in expression between the two conditions. Here too, the Bonferroni correction was applied.

Principal Component Analysis

A principal component analysis (PCA) (Esbensen et al., 2000; Eriksson et al., 2001) was carried out for the genes identified in the ANOVA as having a significantly altered expression in at least one of the deletion strains relative to the reference strain. The PCA was performed in Unscrambler® (version 7.6 by CAMO, Woodbridge, NJ). The data was first mean-centered and divided by the standard deviation to obtain $(\mu,\sigma) = (0,1)$ for each gene. The PCA was validated by the cross validation method.

Reporter Metabolites

Reporter metabolites were determined for each deletion strain using the metabolic network of *S. cerevisiae* (Förster et al., 2003) and the p-values from the pair-wise Student's t-test between the reference strain and each of the mutants. Reporter metabolites are defined as being those metabolites around which the most significant changes in transcription occur (Patil and Nielsen, 2005). They were determined by representing the metabolic network as a bipartite undirected graph and scoring each metabolite based on the normalized transcriptional response of its neighbor enzymes. The top ten high-scoring metabolites where considered to be the reporter metabolites. High-scoring metabolic sub-networks (Patil and Nielsen, 2005) were also determined from the

enzyme interaction network, that is, from a network connecting all enzymes that share a common metabolite. High-scoring sub-networks were identified using a simulated annealing algorithm.

Results

With the purpose of exploring the global physiological and transcriptional effects of deleting key components of the glucose repression pathways in *S. cerevisiae*, we performed aerobic batch cultivations followed by genome-wide transcription analysis of three knockout mutants, *hxk2Δ*, *mig1Δ*, and *mig1Δmig2Δ*. Aerobic batch cultivations were carried out on minimal medium having D-glucose as the sole carbon source. The initial glucose concentration in the cultivations was 40 $g \cdot L^{-1}$ and the genome-wide transcription response was analyzed during the exponential growth phase at a residual glucose concentration of 20 ± 2 $g \cdot L^{-1}$. For the purpose of data analysis, we include here transcriptional data for the reference strain and for the *grr1Δ* mutant already published in Westergaard et al. (2004) (data was generated following the same experimental protocol as for the three strains presented in this work).

Physiological Characterization

Physiological characterization of the reference strain and *grr1Δ* mutant are provided elsewhere (Westergaard et al., 2004) and summarized in Figure 2A,B and in Table II. The three mutant strains *hxk2Δ*, *mig1Δ*, and *mig1Δmig2Δ* are characterized experimentally here (Fig. 2C,D,E,), and a comparison with the reference strain is made whenever necessary.

Similarly to the reference strain and *grr1Δ* mutant, aerobic batch cultivations of the three recombinant strains also showed respiro-fermentative growth. The most noticeable differences relative to the reference strain were found for the *HXK2*-deleted strain (Table II). The maximum specific growth rate was decreased by 30%, while the yield of biomass on glucose was doubled. The yield of ethanol was decreased by 41%, indicating an increased respiratory capacity. The yield of glycerol for the *hxk2Δ* was only 10% of the level found for the reference strain.

For the two other recombinant strains, only the *mig1Δ* recombinant strain showed a slightly altered specific growth rate, increased by 19%, whereas neither the yield of biomass nor that of ethanol was significantly changed relative to the level of the reference strain in any of the two strains, *mig1Δ*

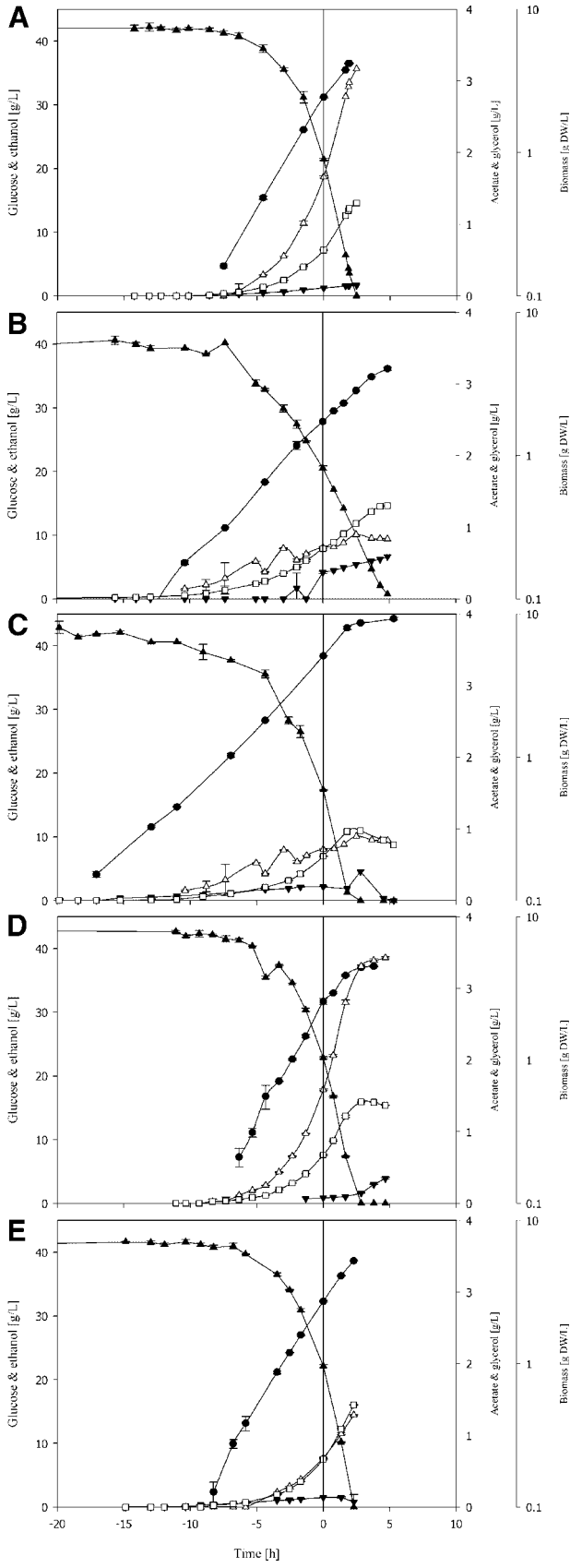

Figure 2. Concentration of substrate, biomass and by-products as a function of time, for the different mutants. The concentrations of glucose (▲), biomass (●), ethanol (□), glycerol (△), and acetate (▼) are presented as a function of time in batch cultivations of (**A**) CEN.PK113-7D *S. cerevisiae*; (**B**) CEN.PK513-3A (*grr1Δ*); (**C**) CEN.PK520-6B (*hxk2Δ*); (**D**) T468 (*mig1Δ*); and (**E**) T475 (*mig1Δmig2Δ*). The time is set to zero at the time point where the samples for whole-genome analysis were withdrawn, which is also indicated by the vertical line in each of the panels.

DOI 10.1002/bit

Table II. Physiological characteristics of strains when cultivated in aerobic batch mode, in triplicates.

Strain	μ_{max}[a] [h^{-1}]	Y_{sx}[b] [g DW · g^{-1}]	Y_{se}[b] [g · g^{-1}]	Y_{sg}[b] [g · g^{-1}]	Y_{sa}[b] [g · g^{-1}]	Invertase activity [mmol glucose · g DW^{-1} · min^{-1}]
CEN.PK113-7D (Ref. Strain)	0.31 ± 0.04	0.10 ± 0.01	0.34 ± 0.01	0.073 ± 0.010	0.0042 ± 0.0008	0.012 ± 0.002
CEN.PK513-3A (*grr1Δ*)	0.23 ± 0.01	0.09 ± 0.01	0.36 ± 0.05	0.031 ± 0.004	0.011 ± 0.002	1.4 ± 0.1
CEN.PK520-6B (*hxk2Δ*)	0.22 ± 0.01	0.20 ± 0.01	0.20 ± 0.06	0.0070 ± 0.0021	n.d.[c]	1.1 ± 0.2
T468 (*mig1Δ*)	0.37 ± 0.02	0.11 ± 0.00	0.37 ± 0.01	0.075 ± 0.010	0.0025[d]	0.025 ± 0.01
T475 (*mig1Δmig2Δ*)	0.27 ± 0.04	0.12 ± 0.01	0.36 ± 0.03	0.054 ± 0.012	n.d.[c]	4.1 ± 0.2

[a]Maximum specific growth rate.
[b]Yield coefficients in g · g^{-1} glucose: Y_{sx}, yield of biomass on glucose; Y_{se}, yield of ethanol on glucose; Y_{sg}, yield of glycerol on glucose; Y_{sa}, yield of acetate on glucose.
[c]n.d.: It was not possible to detect the compound and thus determine the yield coefficient.
[d]Determination only possible for one experiment with this strain.

and *mig1Δmig2Δ*. A comparison of the yields of glycerol revealed a decrease of 26% for the *mig1Δmig2Δ* strain when comparing with the reference strain (Table II).

Invertase activity was determined for all recombinant strains (Table II). Significant increases in invertase activity were found for the strains *hxk2Δ*, *grr1Δ*, and *mig1Δmig2Δ*, which indicated a de-repressed production of the invertase Suc2. The effect of deleting *MIG1* was far less intense and very much comparable with the invertase activity in the reference strain.

Whole-genome Transcription Analysis

Pair-Wise Comparisons and Analysis of Variance

Towards our goal of mapping global transcriptional effects of deleting different components of the glucose repression pathways, we first performed a pair-wise statistical *t*-test to assess significance of differential expression between reference strain and each of the knockout mutants. Using a relatively conservative cut-off, we found from this analysis 76, 35, 10, and 20 genes to display significantly altered expression in the *grr1Δ*, *hxk2Δ*, *mig1Δ*, and *mig1Δmig2Δ* strains, respectively. Lists of genes found from this analysis are given in the Supplementary material 1 together with a discussion of the role of these genes in the metabolism.

Furthermore, in order to identify transcript levels significantly changing across all conditions, an ANOVA test was performed. This test yielded a total of 393 genes found to be significantly down- or upregulated across all conditions, at the chosen level of significance (see Material and Methods). In the set of genes with significantly changed expression profiles, various groups of genes were represented, such as sugar metabolism (*GLK1*, *HXK1*, *MAL11*, *MAL31*, *MAL32*, *FBP26*, *FBP27*, and *SUC2*), amino acid biosynthesis (*IDP2* and *GDH3*), glycogen metabolism (*GLC3*, *GLG1*, *GLG2*, *GPH1*, and *GSY2*), protein biosynthesis (*MRP1*, *MRP49*, *MRPL9*, *MRPL15*, *MRPL38*, and *RPM2*), TCA cycle (*CIT1*, *KGD1*, *LSC1*, *LSC2*, *MDH1*, *SDH1*, *SDH3*, and *SDH4*), respiration (*COX5α*, *COX6*, *COX7*, *ISF1*, *POR1*, *QCR2*, *QCR7*, and *QCR19*), and stress-related genes (*GPX1*, *HSP12*, *HSP26*, *HSP42*, *HSP104*, *UBC5*, and *YGP1*). Besides this, several groups of genes related to transport phenomena were represented: hexose transport (*HXT1*, *HXT2*, *HXT3*, *HXT4*, *HXT6*, *HXT7*, and *HXT16*), amino acid transport (*AGP1* and *GAP1*), ATP synthesis coupled proton transport (*ATP2*, *ATP3*, *ATP4*, *ATP5*, *ATP7*, *ATP14*, *ATP15*, *ATP16*, *ATP17*, *ATP20*, *INH1*, and *PET9*), and genes for other transport functions (*YMC2*, *ATO3*, *MCH5*, *ENB1*, *FRE4*, and *FET4*).

Principal Component Analysis of Genes With Significantly Changed Expression

A PCA was performed for the significant genes determined from the ANOVA in order to ascertain on an overall level how the strains clustered relative to each other and, in more detail, to show which genes influenced the observed clustering the most. For the 393 genes identified by the ANOVA as significantly changed in expression, the triplicate dataset of all five strains were loaded into the PCA. Since the two first principal components captured most of the variance (PC1 captures 63% and PC2 captures 16% of the total variance), our analysis of PCA decomposition only focuses on these two principal components. Regarding the strain-comparison (scores), PCA reveals a co-localization of the *mig1Δ* strain with the reference strain (Fig. 3A), indicating that the transcriptional behavior of the *mig1Δ* strain on a genomic scale was very similar to the reference strain. In contrast to this, the strains *grr1Δ*, *hxk2Δ*, and *mig1Δmig2Δ* all lay apart, suggesting that these strains transcriptionally behaved in a manner different from the reference strain as well as each other (Fig. 3A). When considering the plot of the genes (loadings), one can observe several groupings along both PC1 and PC2 (Fig. 3B). To the left-hand side of the plot (negative values of PC1) a group of hexose transport genes (*HXT1*, *HXT3*, and *HXT4*) and genes related to a range of transport processes (*YMC2*, *ATO3*, *MCH5*, *ENB1*, *FRE4*, and *FET4*) dominate the plot. Additionally, a small group of genes related to rRNA and tRNA (*MRT4*, *UTP14*, *TRM2*, and *UTP30*) contribute to the negative part of PC1.

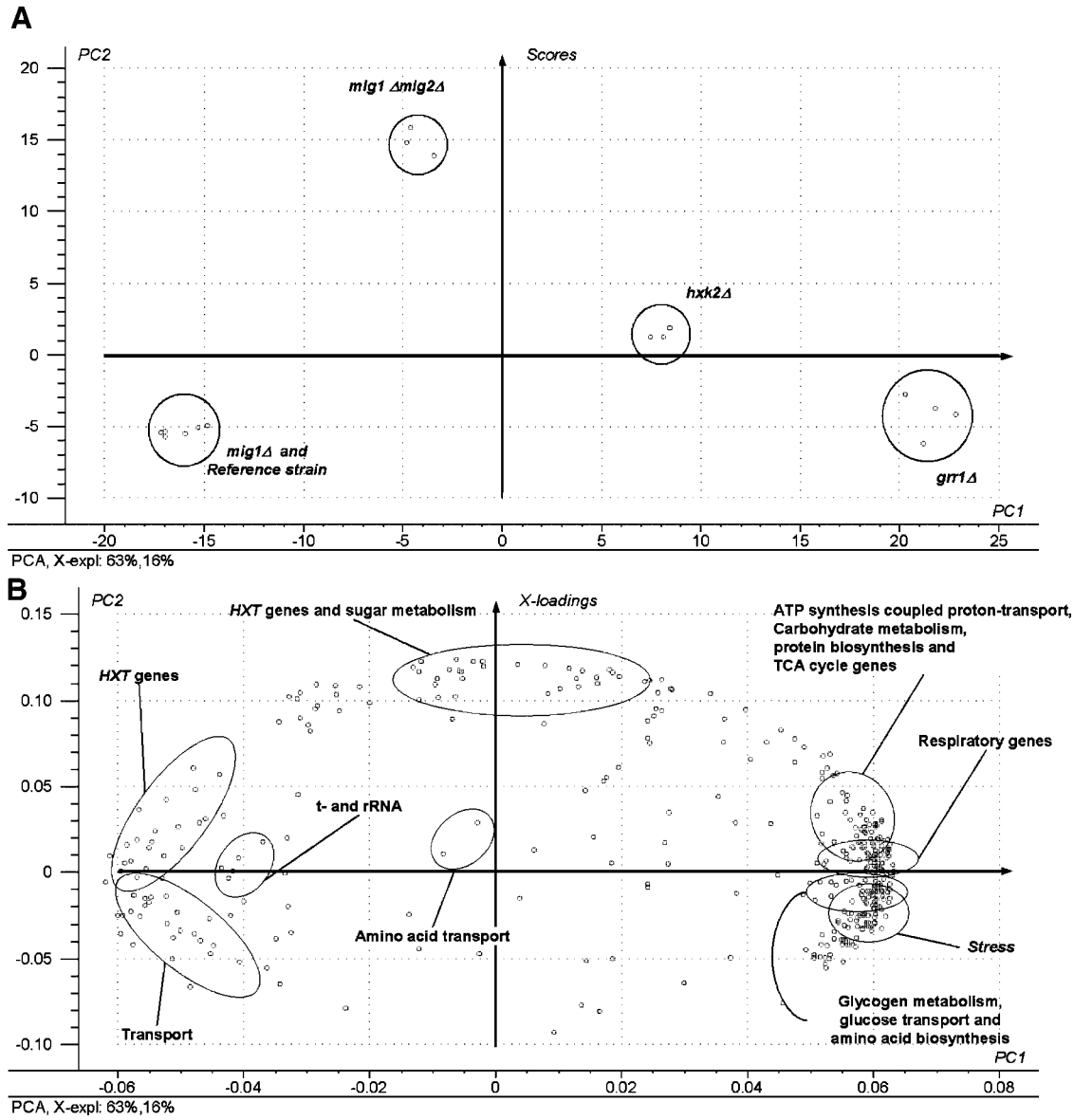

Figure 3. Principal component analysis of strains investigated and the significant genes from the ANOVA. From this, it is possible to determine patterns in expression profiles of the strains as similar profiles will cause strains to co-localize in the score plot (**panel A**). The contribution of each of the individual genes to the two PCs can be assessed from the loadings plot (**panel B**). The areas marked (panel B) represent overrepresentation of the genes specified.

For positive values of PC1, quite a few groups of genes overlap, including ATP synthesis coupled proton transport, carbohydrate metabolism, protein biosynthesis, TCA cycle, respiration, stress, glycogen metabolism, glucose transport (*HXT16*), and genes involved in amino acid biosynthesis (*IDP2* and *GDH3*) (see Section S.7 of the Supplementary material 2 for a more extensive description of the genes involved). Hexose transport genes (*HXT2*, *HXT6*, and *HXT7*) and genes involved in sugar metabolism (*FBP26*, *FBP27*, and *SUC2*) were located in the upper part of the loadings plot (Fig. 3B), and thereby these genes were found to contribute positively to the second principal component (PC2). In the middle of the plot, conferring very little effect on both PC1 and PC2, were two genes involved in amino acid transport (*AGP1* and *GAP1*).

Identification of Reporter Metabolites

In order to further analyze the metabolic effect of disrupting the different components of the glucose repression pathways, we identified the so-called reporter metabolites using a genome-scale metabolic model (Patil and Nielsen, 2005). Reporter metabolites reflect which parts of metabolism are

DOI 10.1002/bit

Table III. Top 10 reporter metabolites.

grr1Δ		*hxk2Δ*		*mig1Δ*		*mig1Δmig2Δ*	
Metabolite	*p*-value	Metabolite	*p*-value	Metabolite	*p*-value	Metabolite	*p*-value
Xanthosine 5′-phosphate	2.78×10^{-3}	alpha-D-Glucose	1.05×10^{-5}	Mannose extracellular	2.94×10^{-3}	Maltose	3.01×10^{-5}
alpha-D-Mannose	3.12×10^{-3}	Glucose extracellular	1.04×10^{-4}	Fructose extracellular	3.58×10^{-3}	alpha-D-Glucose	6.64×10^{-5}
L-Glutamine	3.28×10^{-3}	alpha-D-Mannose	1.05×10^{-4}	Glycerone	1.13×10^{-2}	alpha-D-Mannose	9.18×10^{-4}
Glucose extracellular	5.32×10^{-3}	Fructose extracellular	1.09×10^{-4}	alpha-D-Glutamyl phosphate	1.26×10^{-2}	Mitochondrial orthophosphate	1.36×10^{-3}
D-Fructose	7.28×10^{-3}	D-Fructose	2.13×10^{-4}	Glucose extracellular	1.47×10^{-2}	Mitochondrial CoA	2.11×10^{-3}
sn-Glycerol 3-phosphate	9.71×10^{-3}	Maltose	8.32×10^{-4}	Deoxyuridine	2.14×10^{-2}	D-Fructose	2.30×10^{-3}
Fructose extracellular	9.99×10^{-3}	Mitochondrial H^+	1.05×10^{-3}	L-Tyrosine	2.42×10^{-2}	beta-D-Glucose	4.90×10^{-3}
Glycogen	1.19×10^{-2}	Mannose extracellular	1.32×10^{-3}	Xanthine	2.66×10^{-2}	Fructose extracellular	5.58×10^{-3}
Mannose extracellular	1.43×10^{-2}	Sucrose extracellular	2.69×10^{-3}	alpha-D-Mannose	2.76×10^{-2}	(S)-Dihydroorotate	7.16×10^{-3}
alpha-D-Glucose	1.82×10^{-2}	Mitochondrial orthophosphate	4.40×10^{-3}	alpha-D-Glucose	2.80×10^{-2}	(−)-Ureidoglycolate	1.15×10^{-2}

more affected by a defined perturbation (such as a gene deletion), and analysis of their neighboring enzymes gives a good indication of which pathways/processes are changing, at the transcriptional level, around those metabolites. Table III lists the reporter metabolites identified in each of the four disruption mutants analyzed here and, in the following, we discuss the results for each strain.

The grr1Δ strain. Genes spanning reporter metabolites of the *grr1Δ* strain are over-represented in the Gene Ontology (GO) biological process categories for carbohydrate transport and metabolism, energy reserve metabolism, nucleotide metabolism, amino acid transport and metabolism, and glycerol metabolism. The top-one reporter metabolite is xanthosine 5′-phosphate. Its neighbor enzymes are all related with nucleotide metabolism and significant changes occur, for instances, with *GUA1* and *IMD1*, which are downregulated in this mutant. Both *GUA1* and *IMD1* are known to be repressed, at the transcription level, during nutrient starvation (Escobar-Henriques et al., 2003). L-glutamine appears to be related with changes in amino acid transport and metabolism. Significant downregulation is observed for the amino acid transporters *DIP5*, *GNP1*, *AGP1*, and *GAP1*, and for genes involved in amino acid metabolism (e.g., *TRP2*, *TRP3*, *CPA2*, *ASN2*, and *GLT1*). Neighbor analysis of the reporter metabolite *sn*-Glycerol 3-phosphate gives a clear indication that glycerol-related pathways are derepressed in this mutant, when compared to the reference strain. All other reporter metabolites are related with genes involved in carbohydrate transport and metabolism (such as *HXT1-9*, *HXT16*, *HXK1*, *HXK2*, *GLK1*) and utilization of disaccharides and glycogen (*MAL32*, *NTH2*, *GPH1*, *GLC2*, *GSY1*, and *GSY2*). The list of reporter metabolites clearly points to Grr1 playing a role in regulation of both carbon and nitrogen metabolism.

The hxk2Δ strain. In the case of the *hxk2Δ* mutant, genes spanning reporter metabolites are over-represented in the GO biological process categories for carbohydrate transport and metabolism, disaccharide metabolism, and cellular respiration. Most reporter metabolites are related with genes that have changes in expression of hexose transporters (*HXT1-9*, *HXT16*) and genes involved in disaccharide metabolism (*SUC2*, *MAL32*, *NTH2, FSP2*). Mitochondrial H^+ and orthophosphate are associated with mitochondrial activity and respiration.

The mig1Δmig2Δ strain. For the *mig1Δmig2Δ* strain, there is an over-representation of the GO biological process categories for carbohydrate transport and metabolism (namely tricarboxylic acid cycle, disaccharide metabolism, and hexose transport) and cellular respiration. Reporter metabolites for the *mig1Δmig2Δ* strain highlight (i) the upregulation of both *HXK1* and *HXK2* in the mutant compared to the reference strain, (ii) the higher expression of high-affinity hexose transporters (*HXT2*, *HXT4*, *HXT6*, *HXT7*), (iii) the lower expression of low-affinity hexose transporters (*HXT1*), and (iv) the upregulation of genes involved in the metabolism of disaccharides (*FSP2*, *MAL32*, *SUC2*). Mitochondrial orthophosphate neighbors appear to be related with mitochondria activity and respiration. Mitochondrial CoA is related with the significant upregulation of gene products involved in the tricarboxylic acid cycle. Two reporter metabolites related with the catabolism of nitrogenous compounds show up (S-dihydroorotate and (−)-ureidoglycolate). These metabolites have as neighbors two *URA* genes and two *DAL* genes, respectively, and further analysis of why these metabolites pop-up as metabolic hotspots do require a more integrative analysis of the metabolic network. We have therefore determined high-scoring metabolic subnetworks (Patil and Nielsen, 2005), and this

analysis pointed out that genes that distance one or two reactions from those reporter metabolites are significantly upregulated and mainly involved in TCA cycle, glycolysis, and pentose phosphate pathway. Hence, these two reporter metabolites seem to indicate an overall change in nucleotide metabolism caused by the overall change in the expression level (up-regulation) of genes encoding for TCA cycle, glycolysis, and pentose phosphate pathway.

The mig1Δ strain. Reporter metabolites of the *mig1Δ* strain are more widely distributed among different metabolic processes than for the other mutants, but they are also less significant than reporter metabolites for the other mutants. There is an over-representation of the GO biological process categories for carbohydrate transport and metabolism (namely hexose transport and disaccharide metabolism), and amino acid transport. Similar to what happens with the other mutants, reporter metabolites for the *mig1Δ* strain also highlight changes in the utilization of hexose transporters. Analysis of the neighbor enzymes of deoxyuridine and xanthine seem to indicate that these metabolites are reporting for the different specific growth rate, since they were identified as being growth rate dependent in a dilution series experiment (Regenberg et al., 2006). Analysis of other reporter metabolites indicate a general downregulation in the expression of genes related with amino acid transport and metabolism (e.g., *PRO1*, *PRO2*, *ARO8*, *ARO9*, *TAT1*, *BAP2*, *AGP1*), probably related with nitrogen starvation or with the significant increase in the maximum specific growth rate of the mutant strain.

Influence of Gene Deletion on HXT Genes

In the analyses above the hexose transporter genes, *HXT1* to *HXT9* and *HXT16*, are suggested to have altered expression in several of the mutants. We therefore performed an additional and narrower transcription analysis of these genes, together with the two hexose sensors, *RGT2* and *SNF3* (note that the six remaining hexose transporter genes were either not expressed in any of the experiments—*HXT10*, *HXT12*, and *HXT14*—or they were not represented in the Yeast Genome S98 oligonucleotide array—*HXT11*, *HXT13*, and *HXT15*). This reduced group of 12 genes was investigated using a *p*-value cut-off of 0.02083 after correcting for multiple testing (correction for the 12 genes).

When this cut-off was applied, significant changes were observed in the cases marked in bold in Table IV. Results show that the low affinity transporter *HXT1* has a lower

Table IV. Genes involved in hexose transport and their change in gene expression (relative to the level of the reference strain).

		Fold change[c]				*p*-value[d]					
ORF[a]	Gene name[b]	*grr1Δ*	*hxk2Δ*	*mig1Δ*	*mig1Δ mig2Δ*	*grr1Δ*	*hxk2Δ*	*mig1Δ*	*mig1Δ mig2Δ*	K_M[e]	Description[b]
YHR094C	*HXT1*	−24.6	−6.7	−1.8	−5.6	$\mathbf{8.7 \times 10^{-5}}$	$\mathbf{1.2 \times 10^{-3}}$	2.3×10^{-2}	$\mathbf{1.6 \times 10^{-3}}$	50–100	Low-affinity glucose transporter
YMR011W	*HXT2*	−2.5	7.3	1.3	12.9	$\mathbf{5.5 \times 10^{-4}}$	$\mathbf{9.0 \times 10^{-4}}$	1.7×10^{-1}	$\mathbf{2.3 \times 10^{-5}}$	10	High-affinity glucose transporter 2
YDR345C	*HXT3*	−10.8	−1.5	1.6	−1.1	$\mathbf{2.4 \times 10^{-5}}$	$\mathbf{1.8 \times 10^{-2}}$	$\mathbf{2.6 \times 10^{-3}}$	6.5×10^{-1}	50–100	Low-affinity glucose transporter
YHR092C	*HXT4*	−12.4	2.6	2.4	3.8	$\mathbf{1.8 \times 10^{-3}}$	$\mathbf{1.3 \times 10^{-3}}$	$\mathbf{4.0 \times 10^{-3}}$	$\mathbf{1.1 \times 10^{-4}}$	10	High-affinity glucose transporter
YHR096C	*HXT5*	−1.2	−1.2	−1.5	−1.1	1.0×10^{-1}	2.7×10^{-1}	3.0×10^{-2}	3.2×10^{-1}	10	Hexose transporter with moderate affinity for glucose
YDR343C	*HXT6*	3.9	7.6	1.4	9.0	$\mathbf{6.9 \times 10^{-5}}$	$\mathbf{2.9 \times 10^{-5}}$	$\mathbf{5.2 \times 10^{-4}}$	$\mathbf{1.1 \times 10^{-4}}$	1–2	High-affinity glucose transporter
YDR342C	*HXT7*	3.6	6.5	1.5	7.8	$\mathbf{3.2 \times 10^{-5}}$	$\mathbf{3.2 \times 10^{-5}}$	$\mathbf{7.4 \times 10^{-4}}$	$\mathbf{9.0 \times 10^{-5}}$	1–2	High-affinity glucose transporter
YJL214W	*HXT8*	−1.5	1.7	−1.8	−1.2	6.8×10^{-2}	$\mathbf{1.8 \times 10^{-3}}$	$\mathbf{9.2 \times 10^{-3}}$	4.9×10^{-1}	—	High-affinity hexose transporter
YJL219W	*HXT9*	−1.3	−1.3	−1.3	1.0	7.9×10^{-2}	2.4×10^{-1}	6.4×10^{-2}	7.5×10^{-1}	—	Putative hexose transporter
YJR158W	*HXT16*	43.3	13.8	−1.6	11.3	$\mathbf{2.0 \times 10^{-4}}$	$\mathbf{2.2 \times 10^{-6}}$	2.5×10^{-2}	$\mathbf{4.3 \times 10^{-3}}$	—	Hexose permease
YDL194W	*SNF3*	2.4	1.7	1.3	1.8	$\mathbf{2.3 \times 10^{-4}}$	$\mathbf{6.6 \times 10^{-3}}$	3.5×10^{-1}	2.8×10^{-2}	—	Glucose sensor
YDL138W	*RGT2*	1.1	1.0	1.2	1.1	6.3×10^{-1}	8.1×10^{-1}	3.7×10^{-1}	4.2×10^{-1}	—	Plasma membrane glucose sensor

Bold numbers indicate significant changes observed.
For absolute intensities, see Table S2 in the Supplementary material 1.
[a]Open reading frame.
[b]According to *Saccharomyces* Genome Database Dolinski et al. (2003).
[c]Fold change of gene expression of given gene in the mutant strains compared to expression level in the reference strain.
[d]*p*-value from a *t*-test, indicating the significance of expression change.
[e]K_M [mM] Diderich et al. (2001); Dolinski et al. (2003); Reifenberger et al. (1997).

DOI 10.1002/bit

expression in all strains except for the *mig1Δ* strain. The most pronounced changes were in the *grr1Δ*, *hxk2Δ*, and *mig1Δmig2Δ* strains, with up to a 24-fold reduction of expression in *grr1Δ*. *HXT6*, *HXT7* exhibited a higher expression level in all mutant strains, with increased levels of expression as high as nine- and eightfold in the *mig1Δ mig2Δ* strain. The high affinity transporters *HXT2* and *HXT4* displayed an increased expression level in the *hxk2Δ* and *mig1Δmig2Δ* strains (*HXT4* also in the *mig1Δ* strain), but in the *grr1Δ* strain both genes had a lower expression level. A lower level of *HXT3* expression was observed in the *grr1Δ* and *hxk2Δ* strains, whereas the expression had increased in the *mig1Δ* strain.

In the case of the two glucose sensors, only *SNF3* had significantly changed expression and then only for the *grr1Δ* and *hxk2Δ* strains, where expression had increased about twofold.

Discussion

After analysis of the physiological and genome-wide transcriptional responses for all five strains characterized either in this study or in our previous report (Westergaard et al., 2004), we focus our discussion on: (1) the comparative profiling of all mutants and (2) understanding the role of each deleted component in the cell, particularly in the glucose repression mechanism, and mapping its effects on the metabolism.

Physiologically, we observed that *grr1Δ* and *hxk2Δ* have about the same maximum specific growth rate and show a similar level of glucose repression relief (indicated by the similar value of invertase activity). However, *hxk2Δ* has a higher respiratory capacity, since its biomass yield on glucose is twice the value obtained with all other strains studied, and it is accompanied by a decrease in the ethanol yield. Regarding *mig1Δ* and *mig1Δmig2Δ*, they are physiologically more similar to the reference strain, although the invertase activity in the double mutant is notably higher than in any other case, pointing out for a strong relief of glucose repression mechanisms in the *mig1Δmig2Δ* mutant. We were therefore curious to examine how the strains would cluster at the transcriptional level. Interestingly, we observe from Figure 3 (strain clustering performed by PCA) that the transcriptional grouping of the four mutants is in good agreement with the physiological observations, suggesting that the affected processes are mainly regulated at the transcriptional level. Indeed, transcriptionally, *mig1Δ* and the reference strain cluster together, while all other mutants lay separately. Nevertheless, *grr1Δ* and *hxk2Δ* are relatively close in the second principal component (PC2) axis, suggesting common transcriptional profiles of those genes associated with PC2.

To learn more about the different levels of regulation (transcriptional or post-translational) of the central carbon metabolism in each of the mutants, we combined our transcriptional analysis with in vivo flux profiling reported by Raghevendran et al. (2004). In their study, they performed a phenotypic characterization of the same strains by using ^{13}C-labeled glucose in small-scale reactors, and the physiological parameters (specific growth rates and yields) they observed are comparable to ours. To analyze their data, they performed a PCA decomposition of their flux distributions and found that the mutants group in a similar fashion as we found here, although in their case *grr1Δ* and *hxk2Δ* can be regarded as one cluster. Therefore, it seems that although *grr1Δ* and *hxk2Δ* have different transcriptional programs, phenotypically it leads to similar flux distributions. For the *grr1Δ* strain the decrease in expression of the *HXT* genes results in a decreased glucose in-flux and for the *hxk2Δ* strain the decreased hexokinase activity may result in a decreased glycolytic flux. Thus, in both cases there is a decrease in the glycolytic flux and the phenotypic response at the flux level is therefore similar for the two strains, but the transcriptional response is different. Overall, this comparison therefore supports the observation that the processes mainly affected by the deletion of the components under study are mostly regulated at the transcriptional level.

Focusing on specific genes, it becomes apparent from the PCA analyses that there is an increased expression of genes associated with TCA cycle in both the *grr1Δ* and *hxk2Δ* strains (Fig. 3 and Table S3 in the Supplementary material 2), as well as an increased expression of respiratory and ATP synthesis coupled proton transport genes, the latter also being indicative of increased respiratory capacity. These results are further supported by the pair-wise statistical analysis and by the reporter metabolites.

One important feature of our approach to analyze the transcriptome data was the initial filtering preceding the PCA, by using only genes considered significant from the ANOVA test. This step is crucial for the possibility of identifying the effects that cause the strains to differ. If the PCA was carried out with no prior filtering, both biological and non-biological gene expression variations would be included. In practice, one would still be able to group strains, but the raw ''noisy'' data would have masked the actual biological changes. Since PCA is a decomposition technique that decomposes data according to its variance, non-biological variance should be removed from the initial dataset so that the decomposition will only be performed on the biological variance. This was the rationale behind performing the ANOVA first.

From a global perspective, our analysis shows that glucose repression is intertwined with many other cellular processes. Here, we focus on the effects on metabolism of disrupting the different components of glucose repression pathways. Deletion of both *GRR1* and *HXK2* display a large degree of pleiotropy when the cells are grown at high glucose concentrations. The proteins encoded by these genes clearly have very different functions within the cell, but still the overall phenotypic response is quite similar. Interestingly, our analysis suggests how this can be explained. Disruption

of *GRR1* results in a decreased expression of several of the *HXT* genes resulting in a reduced glucose uptake. This reduced glucose flux leads to de-repression and, therefore, less fermentation and increased respiration (increased expression of TCA cycle genes, respiratory genes, etc.). Hxk2 is believed to be the dominant hexokinase for phosphorylation of glucose and disruption of *HXK2* will therefore result in a substantial decrease in flux through glycolysis. The decreased level of repression of respiration in the *hxk2Δ* mutant may be either due to a regulatory role of Hxk2 or due to the decreased glycolytic flux in this strain. Thus, even though the resulting phenotype of both *grr1Δ* and *hxk2Δ* is similar, the mechanisms governing this are very different. Additionally, both Grr1 and Hxk2 seem to have a regulatory effect on genes related to ATP synthesis coupled to proton transport. Furthermore, deletions of the two genes result in increased expression of a wide range of genes, ranging from carbohydrate transport and metabolism over energy reserve metabolism (*grr1Δ*) and respiration (*hxk2Δ*) to amino acid transport and metabolism (*grr1Δ*). On the other side, deletion of *MIG1* has earlier been shown to have minor effects on phenotype during growth in glucose as the sole carbon source (Gombert et al., 2001). This is confirmed by our analysis.

According to the Kaniak et al. (2004) model, Mig1 is involved in repression of *HXT2* and *HXT4*, and it is interesting to observe that these two genes are significantly upregulated in the *hxk2Δ* mutant. This points to a link between Hxk2 and Mig1, as proposed in Figure 1. Furthermore, our results confirm the cross-talk between the two main glucose sensing pathways as proposed by Kaniak et al. (2004). For example, we find that *MTH1* is upregulated in the *mig1Δmig2Δ* deletion strain.

Mapping of transcriptional changes onto the metabolic network was done by using reporter metabolites. Analysis of reporter metabolites identified hot spots around which most of the metabolic changes occurred, at the transcriptional level, without the need to define what changes in gene expression are or are not significant. Common to all four mutants is the prevailing of metabolites related with sugar transport and sugar metabolism. Reporter metabolites for *grr1Δ*, *hxk2Δ*, and *mig1Δmig2Δ* indicate that in all three strains there is a significant degree of de-repression of genes encoding for products involved in the utilization of alternative carbon sources, which is in good agreement with the measurements of invertase activity presented in Table II. This relief in expression of glucose-repressible genes supports the hypothesis that Grr1, Hxk2, Mig1, and Mig2 are involved in glucose repression signaling pathways. However, only in the case of *hxk2Δ* we can find reporter metabolites involved in respiration, in good agreement with the increased respiratory capacity of this mutant. Mitochondrial metabolites in the *mig1Δmig2Δ* double mutant are mainly associated with an upregulation of genes playing a role in TCA cycle. Nevertheless, for this mutant the increase in expression does not reflect an increased respiratory capacity, when compared with the reference strain. These observations suggest that Hxk2 plays a key role in regulating respiratory genes and/or the overflow metabolism capacity.

In conclusion we demonstrate how genome-wide analysis of several different mutants combined with the use of different bioinformatics analysis methods enables identification of how specific proteins affects different components within the complete system, and hence contributes to mapping of overall interactions between different cellular processes. Our approach of using PCA of genes that are significantly changed in expression enables rapid mapping of mutants, and further analysis using reporter metabolites enables mapping of the large number of genetic changes onto the metabolism.

S.L.W. thanks the Danish Biotechnology Instrument Center (DABIC) for funding. A.P.O. acknowledges Fundação para a Ciência e Tecnologia for funding. Additionally, we acknowledge Thomas Grotkjær for assistance regarding the transcriptome analysis and Kiran Patil for assistance regarding the reporter metabolites algorithm.

Appendixes

Supplementary material is available in the journal webpage and at our website (http://www2.cmb.dtu.dk/additional_material_for_publications/papers/5). Supplementary material 1 presents an additional analysis of the statistically significant changing genes for each pair-wise comparison. Supplementary material 2 lists all the genes considered significant (gene with *p*-values below the cut-offs defined in the text) for the ANOVA and *t*-tests. Gene expression raw data (after normalization) and *p*-values for the ANOVA and for all pair-wise comparisons performed using a Student's *t*-test can be accessed at our website.

References

Ahuatzi D, Herrero P, de la Cera T, Moreno F. 2004. The glucose-regulated nuclear localization of hexokinase 2 in *Saccharomyces cerevisiae* is Mig1-dependent. J Biol Chem 279:14440–14446.

Christensen LH, Schulze U, Nielsen J, Villadsen J. 1995. Acoustic gas analysis for fast and precise monitoring of bioreactors. Chem Eng Sci 50:2601–2610.

Diderich JA, Raamsdonk LM, Kruckeberg AL, Berden JA, van Dam K. 2001. Physiological properties of *Saccharomyces cerevisiae* from which hexokinase II has been deleted. Appl Environ Microbiol 67:1587–1593.

Dolinski K, Balakrishnan R, Christie KR, Costanzo MC, Dwight SS, Engel SR, Fisk DG, Hirschman JE, Hong EL, Nash R, Oughtred R, Theesfeld CL, Binkley G, Lane C, Schroeder M, Sethuraman A, Dong S, Weng S, Miyasato S, Andrada R, Botstein D, Cherry JM. 2003. Gene list with literature curation information from "*Saccharomyces cerevisiae* genome database" ("ORF list and Gene Ontology (GO) annotations" (file: orf_geneontology.tab)). [February 10, 2005].

Dombek KM, Kacherovsky N, Young ET. 2004. The Reg1-interacting proteins, Bmh1, Bmh2, Ssb1, and Ssb2 have roles in maintaining glucose repression in *Saccharomyces cerevisiae*. J Biol Chem 279: 39165–39174.

Dynesen J, Smits HP, Olsson L, Nielsen J. 1998. Carbon catabolite repression of invertase during batch cultivations of *Saccharomyces cerevisiae*:

DOI 10.1002/bit

The role of glucose, fructose, and mannose. Appl Microbiol Biotechnol 50:579–582.

Eriksson L, Johansson E, Kettaneh-Wold N, Wold S. 2001. PCA. Multi- and megavariate data analysis: Principles and applications, Umetrics, Umeå, Sweden, pp. 43–69.

Esbensen KH, Guyot D, Westad F. 2000. Principal component analysis (PCA). Multivariate data analysis—in practice: An introduction to multivariate data analysis and experimental design, CAMO, Oslo, pp. 19–103.

Escobar-Henriques M, Collart MA, Daignan-Fornier B. 2003. Transcription initiation of the yeast *IMD2* gene is abolished in response to nutrient limitation through a sequence in its coding region. Mol Cell Biol 23:6279–6290.

Flick JS, Johnston M. 1991. *GRR1* of *Saccharomyces cerevisiae* is required for glucose repression and encodes a protein with leucine-rich repeats. Mol Cell Biol 11:5101–5112.

Flick KM, Spielewoy N, Kalashnikova TI, Guaderrama M, Zhu Q, Chang HC, Wittenberg C. 2003. Grr1-dependent inactivation of Mth1 mediates glucose-induced dissociation of Rgt1 from *HXT* gene promoters. Mol Biol Cell 14:3230–3241.

Förster J, Famili I, Fu P, Palsson BO, Nielsen J. 2003. Genome-scale reconstruction of the *Saccharomyces cerevisiae* metabolic network. Genome Res 13:244–253.

Gancedo JM. 1998. Yeast carbon catabolite repression. Microbiol Mol Biol Rev 62:334–361.

Gombert AK, Moreira dos SM, Christensen B, Nielsen J. 2001. Network identification and flux quantification in the central metabolism of *Saccharomyces cerevisiae* under different conditions of glucose repression. J Bacteriol 183:1441–1451.

Kaniak A, Xue Z, Macool D, Kim JH, Johnston M. 2004. Regulatory network connecting two glucose signal transduction pathways in *Saccharomyces cerevisiae*. Eukaryotic Cell 3:221–231.

Kim JH, Polish J, Johnston M. 2003. Specificity and regulation of DNA binding by the yeast glucose transporter gene repressor Rgt1. Mol Cell Biol 23:5208–5216.

Klein CJ, Rasmussen JJ, Rønnow B, Olsson L, Nielsen J. 1999. Investigation of the impact of *MIG1* and *MIG2* on the physiology of *Saccharomyces cerevisiae*. J Biotechnol 68:197–212.

Kuchin S, Vyas VK, Kanter E, Hong SP, Carlson M. 2003. Std1p (Msn3p) positively regulates the Snf1 Kinase in *Saccharomyces cerevisiae*. Genetics 163:507–514.

Lakshmanan J, Mosley AL, Özcan S. 2003. Repression of transcription by Rgt1 in the absence of glucose requires Std1 and Mth1. Curr Genet 44:19–25.

Lascaris R, Bussemaker HJ, Boorsma A, Piper M, Van Der SH, Grivell L, Blom J. 2002. Hap4p overexpression in glucose-grown *Saccharomyces cerevisiae* induces cells to enter a novel metabolic state. Genome Biol 4:R3.1–R3.10.

Lascaris R, Piwowarski J, Van Der SH, De Mattos JT, Grivell L, Blom J. 2004. Overexpression of *HAP4* in glucose-derepressed yeast cells reveals respiratory control of glucose-regulated genes. Microbiology 150: 929–934.

Li FN, Johnston M. 1997. Grr1 of *Saccharomyces cerevisiae* is connected to the ubiquitin proteolysis machinery through Skp1: Coupling glucose sensing to gene expression and the cell cycle. EMBO J 16:5629–5638.

Li C, Wong WH. 2001. Model-based analysis of oligonucleotide arrays: Expression index computation and outlier detection. Proc Natl Acad Sci USA 98:31–36.

Mayordomo I, Sanz P. 2001. Hexokinase PII: Structural analysis and glucose signalling in the yeast *Saccharomyces cerevisiae*. Yeast 18:923–930.

Moreno F, Ahuatzi D, Riera A, Palomino CA, Herrero P. 2005. Glucose sensing through the Hxk2-dependent signalling pathway. Biochem Soc Trans 33:265–268.

Moriya H, Johnston M. 2003. Mechanism of signal transduction by the Snf3 and Rgt2 glucose sensors. Yeast 20:S172.

Mosley AL, Lakshmanan J, Aryal BK, Özcan S. 2003. Glucose-mediated phosphorylation converts the transcription factor rgt1 from a repressor to an activator. J Biol Chem 278:10322–10327.

Nath N, McCartney RR, Schmidt MC. 2003. Yeast Pak1 kinase associates with and activates Snf1. Mol Cell Biol 23:3909–3917.

Newcomb LL, Diderich JA, Slattery MG, Heideman W. 2003. Glucose regulation of *Saccharomyces cerevisiae* cell cycle genes. Eukaryot Cell 2:143–149.

Nigavekar SS, Tan YS, Cannon JF. 2002. Glc8 is a glucose-repressible activator of Glc7 protein phosphatase-1. Arch Biochem Biophys 404:71–79.

Oesterhelt C, Thevelein J, Winderickx J, Pardons K. 2003. Glucose-induced cAMP signalling and its sugar phosphorylation requirement in *Saccharomyces cerevisiae*. Yeast 20:S161.

Özcan S. 2002. Two different signals regulate repression and induction of gene expression by glucose. J Biol Chem 277:46993–46997.

Özcan S, Johnston M. 1999. Function and regulation of yeast hexose transporters. Microbiol Mol Biol Rev 63:554–569.

Özcan S, Leong T, Johnston M. 1996. Rgt1p of *Saccharomyces cerevisiae*, a key regulator of glucose-induced genes, is both an activator and a repressor of transcription. Mol Cell Biol 16:6419–6426.

Palomino A, Herrero P, Moreno F. 2005. Rgt1, a glucose sensing transcription factor, is required for transcriptional repression of the *HXK2* gene in *Saccharomyces cerevisiae*. Biochem J 388:697–703.

Patil KR, Nielsen J. 2005. Uncovering transcriptional regulation of metabolism by using metabolic network topology. Proc Natl Acad Sci USA 102:2685–2689.

Polish JA, Kim JH, Johnston M. 2005. How the Rgt1 transcription factor of *Saccharomyces cerevisiae* is regulated by glucose. Genetics 169:583–594.

Raghevendran V, Gombert AK, Christensen B, Kötter P, Nielsen J. 2004. Phenotypic characterization of glucose repression mutants of *Saccharomyces cerevisiae* using experiments with ^{13}C-labelled glucose. Yeast 21:769–779.

Randez-Gil F, Sanz P, Entian KD, Prieto JA. 1998. Carbon source-dependent phosphorylation of hexokinase PII and its role in the glucose-signaling response in yeast. Mol Cell Biol 18:2940–2948.

Regenberg B, Grotkjær T, Winther O, Fausbøll A, Åkesson M, Bro C, Stansen LK, Brunak S, Nielsen J. 2006. Growth-rate regulated genes have a profound impact on interpretation of transcription profiling in *Saccharomyces cerevisiae*. Genome Biol 7:R107.

Reifenberger E, Boles E, Ciriacy M. 1997. Kinetic characterization of individual hexose transporters of *Saccharomyces cerevisiae* and their relation to the triggering mechanisms of glucose repression. Eur J Biochem 245:324–333.

Rolland F, Winderickx J, Thevelein J. 2002. Glucose sensing and signalling mechanisms in yeast. FEMS Yeast Res 2:183–201.

Sanz P, Alms GR, Haystead TA, Carlson M. 2000. Regulatory interactions between the Reg1-Glc7 protein phosphatase and the Snf1 protein kinase. Mol Cell Biol 20:1321–1328.

Schmidt MC, McCartney RR, Zhang X, Tillman TS, Solimeo H, Wolfl S, Almonte C, Watkins SC. 1999. Std1 and Mth1 proteins interact with the glucose sensors to control glucose-regulated gene expression in *Saccharomyces cerevisiae*. Mol Cell Biol 19:4561–4571.

Sutherland CM, Hawley SA, McCartney RR, Leech A, Stark MJ, Schmidt MC, Hardie DG. 2003. Elm1p is one of three upstream kinases for the *Saccharomyces cerevisiae SNF1* complex. Curr Biol 13:1299–1305.

Verduyn C, Postma E, Scheffers WA, van Dijken JP. 1992. Effect of benzoic acid on metabolic fluxes in yeasts: a continuous-culture study on the regulation of respiration and alcoholic fermentation. Yeast 8:501–517.

Westergaard SL, Bro C, Olsson L, Nielsen J. 2004. Elucidation of the role of Grr1p in glucose sensing by *Saccharomyces cerevisiae* through genome-wide transcription analysis. FEMS Yeast Res 5:193–204.

Wodicka L, Dong H, Mittmann M, Ho MH, Lockhart DJ. 1997. Genome-wide expression monitoring in *Saccharomyces cerevisiae*. Nat Biotechnol 15:1359–1367.

Zaldivar J, Borges ACC, Johansson B, Smits H-P, Villas-Bôas SG, Nielsen J, Olsson L. 2002. Fermentation performance and intracellular metabolite patterns in laboratory and industrial xylose-fermenting *Saccharomyces cerevisiae*. Appl Microbiol Biotechnol 59:436–442.